



ELSEVIER

Available online at www.sciencedirect.com

SCIENCE @ DIRECT®

Earth and Planetary Science Letters 237 (2005) 577–589

EPSL

www.elsevier.com/locate/epsl

Rock dilation, nonlinear deformation, and pore pressure change under shear

Yariv Hamiel^{a,b,*}, Vladimir Lyakhovsky^b, Amotz Agnon^a

^a*Institute of Earth Sciences, Hebrew University of Jerusalem, 91904, Jerusalem, Israel*

^b*Geological Survey of Israel, 30 Malkhe Israel St., 95501, Jerusalem, Israel*

Received 2 January 2005; received in revised form 10 June 2005; accepted 24 June 2005

Available online 3 August 2005

Editor: V. Courtillot

Abstract

The dilation of rock under shear gives rise to detectable effects both in laboratory experiments and in field observations. Such effects include hardening due to reduction in pore pressure and asymmetrical distribution of deformation following strike-slip earthquakes. In this paper, we examine the nonlinear poroelastic behavior of isotropic rocks by a new model that integrates Biot's classic poroelastic formulation together with nonlinear elasticity, and apply it to Coulomb failure criterion and pore pressure response to a fault slip. We investigate the poroelastic response of two alternative forms of a non-Hookean second-order term incorporated in the poroelastic energy. This term couples the volumetric deformation with shear strain. Like linear poroelasticity, our model shows an increase of pore pressure with mean stress (according to Skempton coefficient B) under undrained conditions. In addition, in our model pore pressure varies also with deviatoric stresses, where rising deviatoric stresses (at constant mean stress) decreases pore pressure (according to Skempton coefficient A), due to dilatancy. The first version of our model is consistent with a constant A smaller than $1/3$, which is in agreement with the classic work of Skempton, but does not fit well the measured undrained response of sandstones. The second model allows A and B to vary with shear stress, and displays the experimentally observed connection between pore pressure and deviatoric stresses under undrained conditions in Berea and Navajo sandstone samples. Numerical results present in this paper predict dilatancy hardening and suggest that it should be taken into consideration in Coulomb failure stress calculations. We apply our model to the distribution of pore pressure changes in response to a fault slip. Results of numerical simulations of coseismic deformation demonstrate that due to dilatancy regions of decreasing pore pressure are larger relative to regions of increasing pore pressure. The model predictions have significant implications for coseismic water level changes and post-seismic pore pressure diffusion and crustal deformation.

© 2005 Elsevier B.V. All rights reserved.

Keywords: Poroelasticity; Cracked media; Skempton coefficient; Friction coefficient

* Corresponding author. Current address: Institute of Geophysics and Planetary Physics, Scripps Institute of Oceanography, University of California San Diego, La Jolla, CA 92093, USA.

E-mail address: yarivh@ucsd.edu (Y. Hamiel).

1. Introduction

The mechanical interaction between tectonic stresses and pore fluids in crustal rocks is essential for understanding the fundamental processes controlling earthquakes and the seismic cycle. Water level changes induced by an earthquake are a well-known observation [1], and post-seismic deformation was found to be consistent with pore pressure variations in the first period following an earthquake [2,3]. Therefore, the pattern of post-seismic deformation will be strongly affected by the pore pressure distribution after an earthquake. Furthermore, in fault zones pore pressure controls the fault strength [4–7], thus, it plays an essential role in triggering of an earthquake. In this paper we investigate the influence of nonlinear poroelastic behavior of rocks on the fault strength and on the pore pressure distribution after an earthquake.

Observations in both the laboratory and in the earth crust underscore the interaction between deviatoric stresses and pore pressure in porous rocks [8–11]. This interaction has been approached by incorporating the constitutive relations of anisotropic porous media [12]. Yet the deviatoric stresses–pore pressure interaction is significant in isotropic rocks [11]. Therefore, a theoretical study of the interaction between shear stresses and pore pressure in nonlinear isotropic media is needed.

The nonlinearity of the elastic behavior of rocks is a well-established observation at varied scales. Laboratory test on rock samples exhibit nonlinear elastic properties with elastic moduli that depend on the confining pressure [13–16]. Nonlinear elastic behavior of rocks is also reported based on records of ground motion amplification during earthquakes [17]. Recently, the pattern of deformation after the 1997 Manyi earthquake was explained by different elastic moduli for compression and tension [18]. Nonlinear response of brittle rocks, due to the existence of flaws such as microcracks and microvoids, profoundly affects rock strength and elastic properties [19–23]. Another related observation is elastic rock dilatancy under shear loading [11,15,24]. Rock dilation and related pore pressure reduction under undrained conditions has long been recognized [25] and recently confirmed in accurate laboratory experiments [9,11]. In this paper we

present a model that relates the nonlinear elastic behavior of isotropic porous rocks to dilatancy. We examine the poroelastic response of two different non-Hookean second-order terms incorporated in the poroelastic potential. Then, we verify these two models using experimental observations [11]. We apply the new constitutive relations to Coulomb failure criteria and undrained pore pressure response to slip on a strike-slip fault.

2. Theoretical background

2.1. Poroelastic constitutive relations

Pore pressure coupled with matrix deformation was first introduced by Terzaghi [26] with his often quoted one-dimensional consolidation equation that relates the evolution of pore pressure to the stresses in a solid skeleton. Biot [27] was the first to formulate a fully three-dimensional poroelastic theory. His now classic thermodynamic approach derived constitutive relations for isotropic poroelastic solid. Significant progress has been made in developing constitutive and field equations for linear poroelastic media [28–30].

Biot [27,31] wrote the isothermal free energy, F , for poroelastic isotropic media as a second-order expansion with regard to the elastic strain and fluid content:

$$F = \frac{1}{2} \lambda I_1^2 + \mu I_2 + \frac{1}{2} M [\beta I_1 - \zeta]^2, \quad (1)$$

where λ , μ are the Lamé' drained moduli, M and β are the Biot's modulus and coefficient. $I_1 = \varepsilon_{kk}$ and $I_2 = \varepsilon_{ij} \varepsilon_{ij}$ are two invariants of the elastic strain tensor, ε_{ij} (summation notation is used) and ζ is the variation fluid volume per unit volume of the porous material. The total stress tensor, σ_{ij} , and the pore pressure, p , are defined as the first derivative of the energy [32,33]:

$$\sigma_{ij} = \frac{\partial F}{\partial \varepsilon_{ij}} = \lambda I_1 \delta_{ij} + 2\mu \varepsilon_{ij} + \beta M [\beta I_1 - \zeta] \delta_{ij}, \quad (2)$$

$$p = \frac{\partial F}{\partial \zeta} = M [-\beta I_1 + \zeta]. \quad (3)$$

Eq. (2) for, for $\beta=1$, the total stress may be rewritten in terms of effective stress and pore pressure

$$\sigma_{ij} = \sigma_{ij}^e - \beta p \delta_{ij}, \quad (4)$$

where the effective stress, σ_{ij}^e , is

$$\sigma_{ij}^e = \lambda I_1 \delta_{ij} + 2\mu \varepsilon_{ij}. \quad (5)$$

Eq. (4) indicates that the total stress is the difference between the effective stress and pore pressure.

2.2. Undrained pore pressure response

Linear poroelasticity [27,30] predicts that under undrained conditions ($\zeta=0$) the pore pressure change is proportional only to the change in the mean stress, $\sigma_m = -\sigma_{ii}/3$

$$p = B\sigma_m, \quad (6)$$

where B is Skempton's proportionality coefficient. Using Eqs. (2) and (3), B can be written as [33]:

$$B = \frac{\beta M}{K_u}, \quad (7)$$

where $K_u = K + \beta^2 M$ is the undrained bulk modulus, and $K = \lambda + (2/3)\mu$ is the drained bulk modulus. However, based on experiments with clays, Skempton [8] pointed out that the deviatoric stresses can also affect pore pressure under undrained conditions. Based on experimental work, he proposed that the undrained pore pressure buildup during axial loading tests under confining pressure ($\sigma_2 = \sigma_3$, $\tau_d \equiv (\sigma_1 - \sigma_3)/2$) can be written as:

$$dp = B \left(d\sigma_m + 2 \left(A - \frac{1}{3} \right) d\tau_d \right), \quad (8)$$

where A is an additional Skempton coefficient, which relates pore pressure to deviatoric stresses. Henkel [34] and Henkel and Wade [35] generalized Eq. (8) for a three-dimensional loading geometry:

$$dp = B \left(d\sigma_m + \frac{3A-1}{\sqrt{2}} d\tau_{\text{oct}} \right), \quad (9)$$

where the octahedral shear stress is given by

$$\tau_{\text{oct}} = \frac{\sqrt{2}}{3} (S_1^2 - 3S_2), \quad (10)$$

where S_1 and S_2 are two invariants of the stress tensor, defined as [36]: $S_1 = 3\sigma_m$ and $S_2 = \sigma_{11}\sigma_{22} +$

$\sigma_{22}\sigma_{33} + \sigma_{33}\sigma_{11} - \sigma_{12}\sigma_{21} - \sigma_{23}\sigma_{32} - \sigma_{31}\sigma_{13}$. For axial loading under confining pressure ($\sigma_2 = \sigma_3$), $\tau_{\text{oct}} = \frac{2\sqrt{2}}{3} \tau_d$. Note that for triaxial loading tests Eqs. (8) and (9) reduce to linear poroelasticity (Eq. (6)) for $A=1/3$. For $A < 1/3$ the pore pressure is lower than expected from linear poroelasticity (Eq. (6)). This prediction is reasonable since it accounts for the commonly observed dilatation of porous rocks during shear deformation, also known as dilatancy [11,15,25,37]. Recently, Lockner and Stanchits [11] experimentally related the change in pore pressure for axial loading under confining pressure with the mean and differential stress as:

$$dp = \frac{\partial p}{\partial \sigma_m} d\sigma_m + \frac{\partial p}{\partial \tau_d} d\tau_d = B d\sigma_m + \eta d\tau_d, \quad (11)$$

where η is given by

$$\eta = 2B \left(A - \frac{1}{3} \right). \quad (12)$$

The experiments of Lockner and Stanchits [11] reveal that $\eta \leq 0$ for rocks, consistent with $A \leq 1/3$. Moreover, it was found that for sandstones $|\eta|$ increases strongly with τ_d . In the following section, two different forms of an additional non-Hookean terms are discussed, the first provides the dependence of pore pressure on the deviatoric stresses with constant $A \neq 1/3$, while the second form also accounts for the decrease of A (or, increase of $|\eta|$) with τ_d .

3. Nonlinear poroelasticity of isotropic solid

In this section we investigate the undrained to response of a nonlinear isotropic poroelastic material with energy potential that includes one of the two alternative non-Hookean second-order terms, N_1 or N_2 . Nonlinear stress-strain relationships of elastic and poroelastic rocks can be approximated by including higher-order terms of the strain tensor in the elastic energy expression [38–40]. Such models are successful for rock deformation under high pressures [41], but failed explaining nonlinearity for small elastic deformation in shear. The nonlinear elastic moduli of the Murnaghan model [39] estimated from stress-induced seismic anisotropy are three to four orders of magnitude higher than the Lamé moduli [42]. These

results are not realistic in comparison to those obtained from static experiments. Moreover, the model with high order terms cannot explain the abrupt change in the elastic moduli when deformation changes from compression to tension during experiments on rocks [23,43]. It also fails to provide an appropriate explanation for experimentally observed nonlinear resonance of elastic waves in rocks [16]. In several previous works, the nonlinear elastic behavior was related to opening and closure of microcracks under variable loads [20,43,44]. Lyakhovsky and Myasnikov [45] and Lyakhovsky et al. [43,46] suggested that this feature might be accounted by introducing a non-analytical second-order term with non-integer power of strain invariant in the energy potential (Eq. (1)). Energy expressions with non-integer power of state variables are common for many well-known nonlinear systems, e.g., Hertzian theory for elastic deformation of a granular media [38] or Van der Waals energy equation for a non-ideal gas. Following a general approach of nonlinear behavior of the poroelastic isotropic solid [38], the free energy can be written as

$$F = \frac{1}{2} \lambda I_1^2 + \mu I_2 + \frac{1}{2} M \cdot [\beta I_1 - \zeta]^2 + N(I_2, I_2, I_3), \quad (13)$$

where $I_1 = \varepsilon_{kk}$ and $I_2 = \varepsilon_{ij} \varepsilon_{ij}$ are the same two invariants of the elastic strain tensor used in Eq. (1), and $I_3 = \det(\varepsilon_{ij})$ is a third invariant of the elastic strain tensor. N is a non-Hookean term incorporated in the energy in order to describe nonlinear phenomena. We assume that the pore pressures remain within the range of linear compressibility, and therefore, higher-order terms of ζ are not included in the free energy (Eq. (13)). The energy potential (Eq. (13)) is formulated in terms of strain invariants I_1 , I_2 , and I_3 , thus the material is referred here as isotropic. However, any non-hydrostatic load leads to a stress-induced anisotropy and seismic anisotropy [42,47,48]. Similarly to Eq. (2) the stress–strain relation of nonlinear poroelastic medium is

$$\sigma_{ij} = \lambda I_1 \delta_{ij} + 2\mu \varepsilon_{ij} + \beta M [\beta I_1 - \zeta] \delta_{ij} + \frac{\partial N}{\partial \varepsilon_{ij}}. \quad (14)$$

Lyakhovsky et al. [43] discuss two different forms of a non-Hookean second-order term derived

for the elastic material with non-interacting randomly oriented cracks embedded inside a homogeneous dry matrix. The solution for the elastic energy of such materials was derived using the self-consistent scheme of Budiansky and O’Connell [49], accounting for the elastic energy change associated with crack opening and closure in response to a reverse of the stress component normal to the crack. Two different forms for non-Hookean second-order terms were suggested. In one case a two-dimensional model of the cracked solid was considered, while in the other, the energy potential was derived for a three-dimensional solid with randomly distributed penny-shape cracks. Following Lyakhovsky et al. [43], we examine the poroelastic response of two alternative versions of a non-Hookean second-order term (N_1 , N_2) added to the energy

$$N_1 = -\gamma' I_1 \sqrt{I_2 - \frac{1}{3} I_1^2}, \quad (15a)$$

$$N_2 = -\gamma I_1 \sqrt{I_2}, \quad (15b)$$

where γ (or γ') is a non-analytical strain coupling modulus which accounts for the nonlinearity of the material. Eq. (15a) was derived from a two-dimensional solution of the elastic energy change associated with and crack opening due to a tensile stress applied perpendicular to the cracks [43]. Eq. (15b) approximates well empirical energy changes in a three-dimensional geometry with cracks oriented either perpendicular to the maximum tension axis or perpendicular to the maximum compression axis [43]. Each term in Eq. (15) incorporates nonlinear elasticity, even for an infinitesimal strain, and enable simulating an abrupt change of the apparent elastic moduli when the loading reverses from compression to tension, a widely reported feature of a cracked solid [20,43,44]. Eqs. (15a) and (15b) give rise to two alternative forms of the coupling between the volumetric strain (I_1) and the shear strain, which contribute to the second strain invariant (I_2), and cause the stress–strain relations to be nonlinear even for small deformations. This coupling between volumetric deformation and shear strain leads, via Eq. (3), to the connection between pore pressure and shear stress.

3.1. Non-Hookean term N_1 : constant Skempton coefficients

In this section, we discuss the equations of state and the poroelastic response of a medium, using the non-Hookean second-order term N_1 Eq. (15a). Similarly to Eq. (2), the stress–strain relation can be written as

$$\sigma_{ij} = \left(\lambda - \gamma' \left(\frac{1}{\xi^*} - \frac{\xi^*}{3} \right) \right) I_1 \delta_{ij} + (2\mu - \gamma' \xi^*) \varepsilon_{ij} + \beta M [\beta I_1 - \zeta] \delta_{ij}, \quad (16)$$

where ξ^* is a particular invariant of the strain tensor, $\xi^* = I_1 / \sqrt{I_2 - \frac{1}{3} I_1^2}$. For all deformations, ξ^* varies between $\xi^* \rightarrow -\infty$ for pure compaction to $\xi^* \rightarrow +\infty$ for pure tension. A value of $\xi^* = 0$ corresponds to pure shear or zero volumetric strain ($I_1 = 0$). Since we did not modify the dependence of the energy on the fluid content variable, ζ , Eq. (3) for pore pressure is still valid. Similarly to Eq. (4), the equation for the total stress Eq. (16) may be rewritten in terms of effective stress and pore pressure, where the effective stress is given by

$$\sigma_{ij}^e = \left(\lambda - \gamma' \left(\frac{1}{\xi^*} - \frac{\xi^*}{3} \right) \right) I_1 \delta_{ij} + (2\mu - \gamma' \xi^*) \varepsilon_{ij}. \quad (17)$$

The stress–strain relation Eq. (17) can be rewritten to mimic the usual form of Hooke's law by introducing strain dependent effective moduli

$$\lambda^e = \lambda - \gamma' \left(\frac{1}{\xi^*} - \frac{\xi^*}{3} \right); \quad \mu^e = \mu - \frac{1}{2} \gamma' \xi^*. \quad (18)$$

Note that Eqs. (16) and (17) reduce to the equations of state developed by Biot [27,31] for linear poroelastic media (Eqs. (2), (4)) in the limit of vanishing the strain coupling modulus. ($\gamma = 0$).

Our model predicts that pore pressure depends not only on the mean stress, as in linear poroelasticity, but also on the deviatoric stresses. In the present work, we adopt the format of Eq. (11) as was written by Lockner and Stanchits [11] and generalize it to a three-dimensional state of stresses:

$$dp = \frac{\partial p}{\partial \sigma_m} d\sigma_m + \frac{\partial p}{\partial \tau_{\text{oct}}} d\tau_{\text{oct}} = B d\sigma_m + A' d\tau_{\text{oct}}. \quad (19)$$

Following Henkel [34] and Henkel and Wade [35], A' can be written as:

$$A' = \frac{3A - 1}{\sqrt{2}} B. \quad (20)$$

For axial loading under confining pressure A' reduces to $A' = \frac{3}{2\sqrt{2}} \eta$. In order to find Skempton coefficients, A (or A') and B , we differentiate pore pressure with respect to σ_m and τ_{oct} (see Appendix A for details)

$$A' = \left. \frac{\partial p}{\partial \tau_{\text{oct}}} \right|_{\sigma_m} = \frac{-\sqrt{3} \beta M \gamma'}{2\mu K_u - \gamma'^2}, \quad (21)$$

$$B = \left. \frac{\partial p}{\partial \sigma_m} \right|_{\tau_{\text{oct}}} = \frac{\beta M}{K_u - \gamma'^2 / 2\mu}. \quad (22)$$

Unlike linear poroelasticity, the coefficient A' was found to be non-zero, where in this model with N_1 the poroelastic coefficients are constants. Positive γ provides negative A' , which corresponds to a dilatant response to increasing deviatoric stresses, due to crack opening. Note that if $\gamma = 0$ then $A' = 0$, and B reduces to the linear poroelastic form (Eq. (7)). Eqs. (21) and (22) reveal that A' is proportional to B

$$A' = -\frac{\sqrt{3} \gamma'}{2\mu} B. \quad (23)$$

Using Eqs. (23) and (20), Skempton coefficient, A , can be written as:

$$A = \frac{1}{3} - \frac{\gamma'}{\sqrt{6}\mu}. \quad (24)$$

This result of constant A , smaller than 1/3, in isotropic medium is in agreement with the classic work of Skempton [8], Henkel [34], Henkel and Wade [35], and is usually assumed in models that takes into account the effects of deviatoric stresses on pore pressure response [9,10].

3.2. Non-Hookean term N_2 : variable Skempton coefficients

The stress–strain relations of a poroelastic medium, using the non-Hookean second-order term N_2 (Eq. (15b)), was described by Hamiel et al. [50]. Here we briefly discuss these relations, and further develop the poroelastic response to a three-dimensional state

of stresses. Using N_2 (Eq. (15b)), the stress–strain relation can be written as

$$\sigma_{ij} = \left(\lambda - \frac{\gamma}{\xi} \right) I_1 \delta_{ij} + (2\mu - \gamma\xi) \varepsilon_{ij} + \beta M [\beta I_1 - \zeta] \delta_{ij}, \quad (25)$$

where ξ is given by a strain invariant ratio $I_1/\sqrt{I_2}$. For all deformations ξ ranges between $-\sqrt{3} \leq \xi \leq \sqrt{3}$, where for isotropic compaction $\xi = -\sqrt{3}$, for isotropic dilation $\xi = \sqrt{3}$, and for pure shear or zero volumetric strain ($I_1=0$), $\xi=0$. Since we did not introduce any new term depending on fluid content (ζ) to the poroelastic energy, expression Eq. (3) for pore pressure has the same form also in this model. Similar to the model in Section 3.1, Eq. (25) reduces to the equations of state developed by Biot [27,31] for linear poroelastic media when $\xi \rightarrow 0 - \gamma=0$. In the same manner as Section 3.1 (Eqs. (21) and (22)), we calculated each poroelastic coefficient in Eq. (19) (see Appendix A for details). Unlike the previous section, A' varies with ξ

$$A' = \frac{\partial p}{\partial \tau_{\text{oct}}} \Big|_{\sigma_m} = \frac{-\sqrt{3}\beta M}{2\left(\mu - \frac{1}{2}\gamma\xi\right)\sqrt{\frac{1}{\xi^2} - \frac{1}{3}} + \frac{(6\mu - \gamma\xi^3)\left(K_u - \gamma\left(\frac{1}{\xi} + \frac{\xi}{3}\right)\right)}{3\gamma\xi^3\left(\frac{1}{\xi^2} - \frac{1}{3}\right)^{\frac{3}{2}}}}, \quad (26)$$

where for pure compaction ($\xi = -\sqrt{3}$), $A'=0$, and $A' = \frac{-\sqrt{3}\beta M\gamma}{2\mu K_u - \gamma^2}$ for small mean stresses relative to deviatoric stresses ($\xi \rightarrow 0$). A' can be estimated by a linear interpolation with respect to ξ between $\xi=0$ and $\xi = -\sqrt{3}$:

$$A' \cong \frac{-\beta M\gamma}{2\mu K_u - \gamma^2} (\xi + \sqrt{3}). \quad (27)$$

In the case of small nonlinearity, i.e. $K_u \gg \gamma$, Eq. (27) can be expressed as:

$$A' \cong \frac{-\gamma B}{2\mu} (\xi + \sqrt{3}). \quad (28)$$

$|A'|$ in this model strongly increases with ξ , and therefore pore pressure decreases concomitantly. This reduction in pore pressure occurs by dilatancy represented by the non-analytical term (N_2) in the

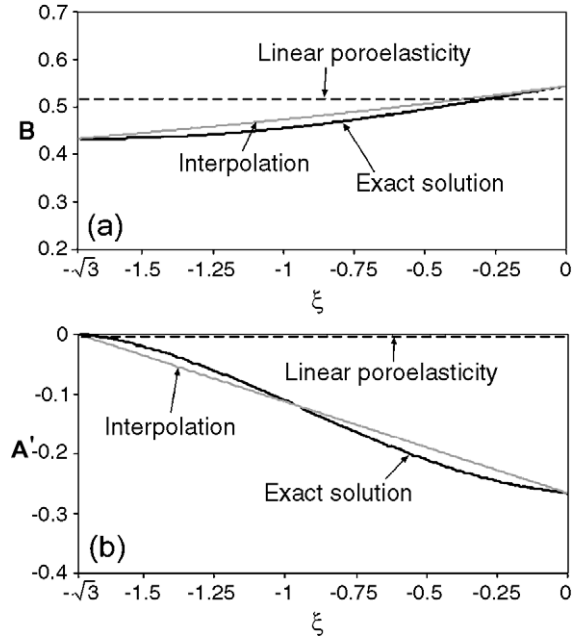


Fig. 1. Exact analytical (Eqs. (26), (30)) versus approximate solution by interpolation (Eqs. (27), (31)) of Skempton coefficient B (a) and A' (b) as a function of $\xi (= I_1/\sqrt{I_2})$ in the present model with the non-Hookean term N_2 , and their values from linear poroelasticity calculations, using Navajo sandstone poroelastic moduli (for model coefficients see Table 1).

poroelastic energy. Owing to the relation between A' and A (Eq. (20)) and using Eq. (28) Skempton coefficient, A , can be written as:

$$A \cong \frac{1}{3} \left[1 - \frac{\gamma}{\sqrt{2}\mu} (\xi + \sqrt{3}) \right]. \quad (29)$$

In the present model A' vanishes (or, $A=1/3$) in the linear limit ($\gamma=0$), or for pure compaction ($\xi = -\sqrt{3}$). Since A' depends on the strain diagonality ξ , then for triaxial loading (with initial conditions of pure compaction) $|A'|$ increases with ξ until failure.

Similarly to Eq. (26) we write Skempton coefficient B , as

$$B = \frac{\partial p}{\partial \sigma_m} \Big|_{\tau_{\text{oct}}} = \frac{\beta M}{K_u - \gamma \left[\left(\frac{1}{\xi} + \frac{\xi}{3} \right) - \frac{6\xi^3 \left(\mu - \frac{1}{2}\gamma\xi \right) \left(\frac{1}{\xi^2} - \frac{1}{3} \right)^2}{6\mu - \gamma\xi^3} \right]}. \quad (30)$$

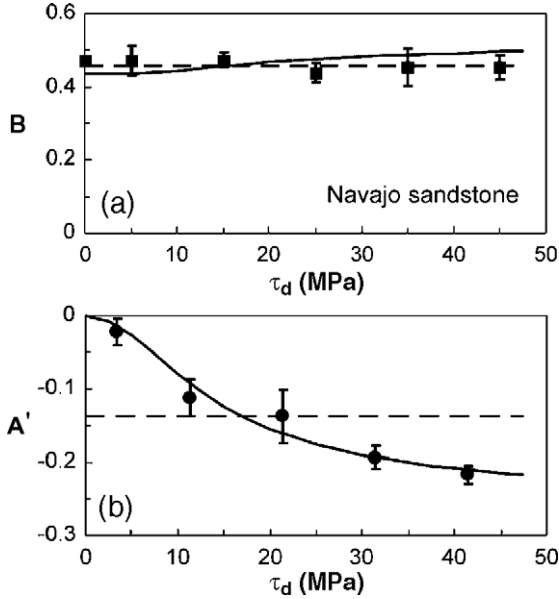


Fig. 2. Measured poroelastic coefficients B and A' (symbols) for Navajo sandstone [11] compared with the calculated curves using the non-Hookean terms N_1 (dashed line) and N_2 (thick line), for different values of $\tau_d (= \frac{1}{2}(\sigma_1 - \sigma_3))$. In these calculations $\sigma_3^c = 17$ MPa (initial pore pressure $p = 3$ MPa) and we used the poroelastic moduli listed in Table 1.

The denominator of Eq. (30) equals $K_u + \frac{2}{\sqrt{3}}\gamma$ for pure compaction ($\zeta = -\sqrt{3}$), and $K_u - \frac{\gamma^2}{2\mu}$ for pure shear ($\zeta = 0$). Therefore, by interpolation of B^{-1} with respect to ζ between $\zeta = 0$ and $\zeta = -\sqrt{3}$, B can be estimated as

$$B \cong \frac{\beta M}{K_u - \gamma \left[\left(\frac{2}{3} + \frac{\gamma}{2\sqrt{3}\mu} \right) \zeta + \frac{\gamma}{2\mu} \right]}. \quad (31)$$

B in our model is found to be almost constant, increasing slightly with ζ . Again, if nonlinearity is assumed to be small, i.e., $K_u \gg \gamma$, then B from linear poroelasticity is retrieved as

$$B \cong \frac{\beta M}{K_u}. \quad (32)$$

Fig. 1 shows the exact analytical solution (Eqs. (26), (30)) and interpolation (Eqs. (27), (31)) for B (Fig. 1a) and A' (Fig. 1b), and their values from linear poroelasticity, with Navajo sandstone poroelastic moduli (see Section 4).

4. Comparison with experimental data

Rock dilation under shear and the related pore pressure reduction under undrained conditions has long been recognized, but only recently confirmed in laboratory experiments [11] with complete description of the experimental setup and the results needed for model verification. Lockner and Stanchits [11] measured the undrained response of Berea and Navajo sandstones to changes in mean and deviatoric stresses for triaxial loading. Similarly to Lockner and Stanchits [11], we examine the change of pore pressure under undrained conditions at different deviatoric stresses. We present here simulations using the two different forms of the non-Hookean terms (Eqs. (15a), (15b)) for triaxial loading under undrained conditions ($\sigma_2 = \sigma_3 = \text{const.}$, $\zeta = 0$). Each poroelastic coefficients in Eq. (19) were calculated, using the non-Hookean terms N_1 and N_2 . In the first case (N_1) the poroelastic coefficients depend only on the material properties and are not related to the applied load (Eqs. (21) and (22)). In the second case the poroelastic coeffi-

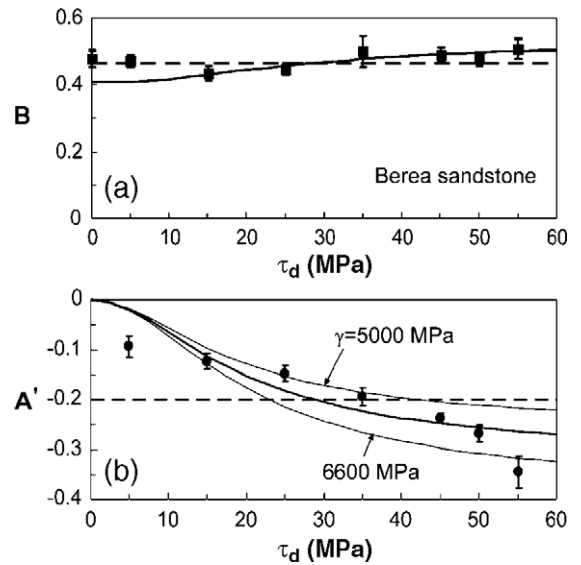


Fig. 3. Measured poroelastic coefficients B and A' (symbols) for Berea sandstone [11] compared with the calculated curves using the non-Hookean terms N_1 (dashed line) and N_2 (thick line), for different values of $\tau_d (= \frac{1}{2}(\sigma_1 - \sigma_3))$. In these calculations $\sigma_3^c = 17$ MPa (initial pore pressure $p = 3$ MPa) and we used the poroelastic moduli listed in Table 1. Thin lines in (b) indicate calculations with different values of γ (5000 and 6600 MPa). Note that A' decreases with γ .

coefficients depend on the load through the strain invariant, ξ (Eqs. (26) and (30)), that for a given stress tensor is obtained by numerical solution of a polynomial equation (Eq. (3) in [46]).

The experimental data reported by Lockner and Stanchits [11] showed that Skempton coefficients vary with the deviatoric stresses, suggesting that our second model with N_2 (Section 3.2) is more appropriate in describing the experimental data. Figs. 2 and 3 show the measured poroelastic coefficients A' and B for Navajo (Fig. 2) and Berea (Fig. 3) sandstones samples from Lockner and Stanchits [11] compared with the calculated curves with the non-Hookean terms N_1 (Section 3.1) and N_2 (Section 3.2). In these calculations we have adopted Terzaghi's assumption ($\beta=1$) and used the poroelastic moduli listed in Table 1. Similar results can be obtained by choosing different values of β and M . Figs. 2 and 3 reveal that Skempton coefficient, B , in our model is about constant or slightly increases with shear stress, while A' strongly decreases with shear stress. We study the sensitivity of the calculated poroelastic coefficients A' and B to the nonlinear strain coupling modulus, γ . The calculations show that, while B is only slightly affected by nonlinearity (not shown here), A' strongly decreases with γ (Fig 3b). Figs. 2 and 3 demonstrate a good agreement between the measured values of undrained poroelastic coefficients for Navajo and Berea sandstones samples and the theoretical curve with the non-Hookean term N_2 . Lockner and Stanchits [11] estimated that η_0 (the value of η at zero differential stress) for Berea sandstone sample is -0.075 . This might be due to anisotropy inherent in the Berea sandstone samples [11]. The non-zero value of η_0 is equivalent to non-zero value of A' . This could be the reason that our model with N_2 does not accurately match the measured A' for the Berea sandstone at very low deviatoric stresses,

since our model assume isotropic poroelasticity and $A'=0$ for pure compression.

5. Model applications

5.1. Coulomb failure criterion

In this section we explore the influence of the undrained response of the model with the non-Hookean term N_2 (Section 3.2) on the Coulomb failure criterion. Rock failure can be predicted by the Coulomb failure criterion [36]. Using this criterion, the change in proximity to failure is defined as [51,52]:

$$\Delta\text{CFS} = \Delta\tau - \mu_s(\Delta\sigma_n - \Delta p), \quad (33)$$

where ΔCFS is the change in Coulomb failure stress, $\Delta\tau$ is shear stress change on the fault plane, $\Delta\sigma_n$ is the normal stress change across the fault plane, Δp is pore pressure change, and μ_s is the coefficient of static friction. Positive values of ΔCFS imply that the rock is closer to failure, whereas, negative values imply that the rock is farther away from failure. Substituting Eq. (19) into Eq. (33), ΔCFS can be written as

$$\Delta\text{CFS} = \Delta\tau - \mu^a \Delta\sigma_n, \quad (34)$$

where the apparent friction coefficient, μ^a , is given by:

$$\mu^a = \mu_s \left(1 - B \frac{\Delta\sigma_m}{\Delta\sigma_n} + |A'| \frac{\Delta\tau_{\text{oct}}}{\Delta\sigma_n} \right). \quad (35)$$

The last term in Eq. (35) accounts for an increase in the apparent friction coefficient due to dilatancy expressed by the shear-dilation coupling term in the poroelastic energy (Eqs. (15a), (15b)). Fig. 4 shows the increase in the apparent friction coefficient with γ , the modulus of the non-Hookean term N_2 . In the calculations presented in Fig. 4 we used the poroelastic coefficients of Berea sandstone (for model coefficient see Table 1), and assume representative value of $\mu_s=0.75$ [36,51,53]. We also assume that $\Delta\sigma_n=\Delta\sigma_m$. This assumption which leads to constant apparent friction coefficient, $\mu^a=\mu_s(1-B)$, in linearly poroelastic rock, has been widely discussed in studies of rock failure using the Coulomb failure criterion [51,52,54]. As shown in Fig. 4, the apparent friction

Table 1
Model coefficients for the different simulations

Sandstone type	Non-Hookean term	λ (MPa)	μ (MPa)	γ (or γ') (MPa)	M (MPa)
Navajo sandstone	N_1	8000	8500	2950	11000
	N_2	8000	8500	4800	14700
Berea sandstone	N_1	8000	8500	4200	11000
	N_2	5000	8500	5800	12000

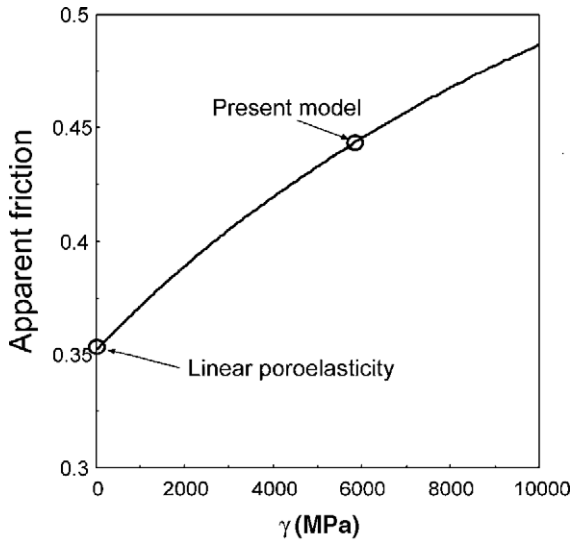


Fig. 4. Apparent coefficient of friction, μ^a , versus the non-Hookean term (N_2) moduli, γ . In these calculations we used the poroelastic moduli of Berea sandstone (for poroelastic moduli see Table 1) and $\mu_s=0.75$. We also assumed that $\Delta\sigma_n=\Delta\sigma_m$. In Berea sandstone the apparent strengthening by dilatancy in the present model is about 25% compared to linear poroelasticity.

coefficient of Berea sandstone is higher by about 25% than that calculated from linear poroelasticity. This increase corresponds to dilatancy hardening in undrained conditions.

5.2. Undrained pore pressure response to a slip on a strike-slip fault

The nonlinear poroelastic model (Section 3.2) is now applied to simulate the undrained pore pressure change in response to a slip event on a strike-slip fault. In order to simulate this response, we used the numerical code developed by Hamiel et al. [55], which is based on an explicit finite element method similar to the Fast Lagrangian Analysis of Continua (FLAC) algorithm [56,57]. We examine the behavior of high-porosity rock at shallow depth, using the poroelastic properties of Berea sandstone that were presented in the previous section. These simulations indicate that the non-Hookean term in the free energy is significant in the calculation of pore pressure changes after slip. Fig. 5 shows a comparison between simulation of coseismic pore pressure changes for a right lateral slip of 1 m on a strike-slip fault of 100

km long, using linear poroelasticity (Fig. 5a) and the present model (Fig. 5b). Under linear poroelasticity, the map of pore pressure change contains four symmetrical quadrants alternating in their sign (Fig. 5a). This symmetry is broken when $\gamma>0$. Due to dilatancy ($\gamma>0$), the areas where pore pressure decreases are enlarged compared to linear poroelasticity (Fig. 5b). As a result, different patterns of fluid flow and poroelastic rebound, following an earthquake, are expected from linear poroelasticity and the present model. This may potentially affect the spatial and temporal distribution of aftershocks.

A first step to incorporate deviatoric stresses–pore pressure interaction in solving pore pressure response to a slip event on a fault was made by Wang [9] and Ge and Stover [10]. These authors argued that the coseismic water level changes observed near the fault trace associated with the Parkfield, December 20, 1994, earthquake can be explained better by calcula-

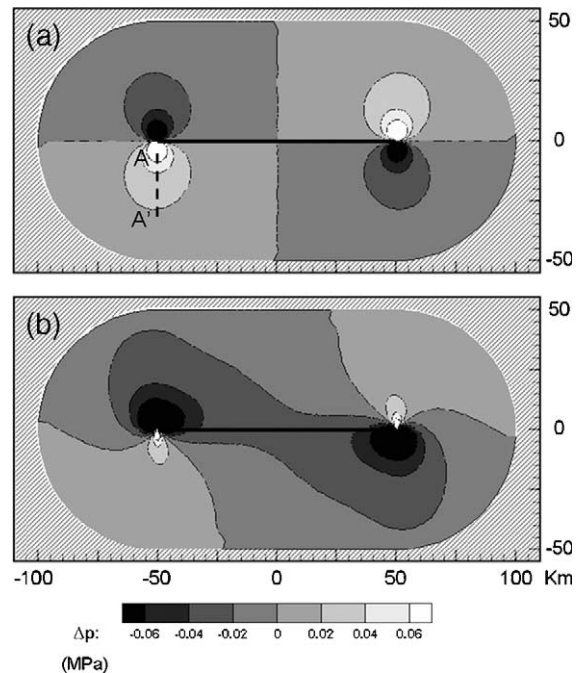


Fig. 5. Distribution of pore pressure change (Δp , in MPa) due to a right lateral slip of 1 m on a strike-slip fault (thick black line) of 100 km long in Berea sandstone using linear poroelasticity (a) and the present model (for poroelastic moduli of Berea sandstone see Table 1). Pore pressure changes along section A–A' (dashed line) are presented in Fig. 6.

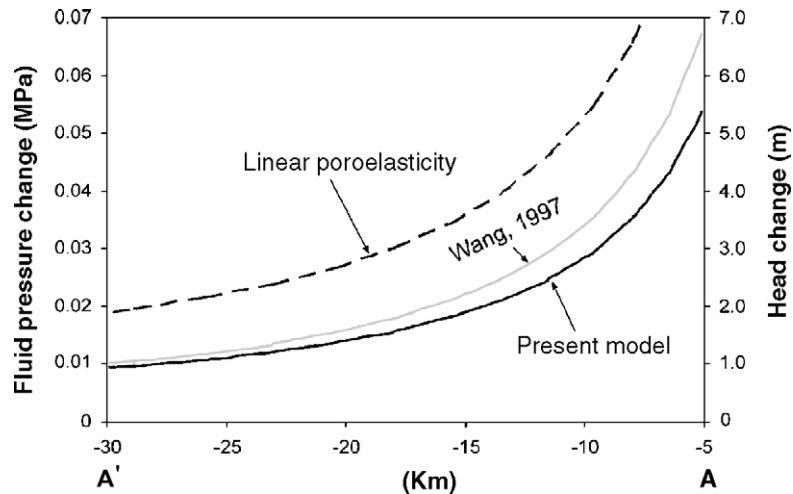


Fig. 6. Calculated pore pressure and hydraulic head changes in linear poroelasticity, our model, and Wang's [9] model, along a section marked in Fig. 5 ($A-A'$). Head change was calculated using $\Delta h = \Delta p / \rho g$.

tions with Skempton coefficient $A < 1/3$ than with by those predicted by linear poroelasticity ($A = 1/3$). However, the solution adopted by Wang [9] and Ge and Stover [10] neglects the relation between deviatoric stresses and pore pressure in the poroelastic constitutive relations [10], possibly a sufficient approximation for small coupling of shear and pore pressure. Here we took a further step toward an internally consistent theory of poroelasticity. Fig. 6 compares calculated pore pressure and hydraulic head changes in linear poroelasticity, our model, and Wang's [9] model, along a section marked in Fig. 5. Head change was calculated by $\Delta h = \Delta p / \rho g$ where h is the hydraulic head, ρ is the density of water, and g is the gravitational acceleration. As shown in Fig. 6, the linear elastic solution predicts a higher response at all simulated distances from the fault tip, a manifestation of dilatancy. The far field solutions of the two other models are indistinguishable. However, Wang's [9] approximate solution overestimates pore pressure increase and underestimates pore pressure decrease around the fault. To summarize, we argue that the solution given by Wang [9] and Ge and Stover [10] can approximate well pore pressure response to slip relatively far from the fault tips, whereas near the fault tips (in the present simulation, $\sim 20\%$ from the fault length) pore pressure increase should be detectably lower (and pore pressure decrease should be detectably higher).

6. Discussion

We have presented here a model that integrates the classic poroelasticity theory of Biot [27] together with nonlinear elasticity. Our formulation provides an internally consistent solution for coupling of shear and pore pressure. In the present paper, we derived general constitutive poroelastic relations so that we can take into account the connection between pore pressure and deviatoric stresses. We investigated the poroelastic response of two different non-Hookean second-order terms, N_1 (Eq. (15a)) and N_2 (Eq. (15b)) added to the energy potential (Eq. (13)). These terms couple the shear strain with the volumetric deformation. As in linear poroelasticity, both models show an increase of pore pressure with mean stress (according to Skempton coefficient B) under undrained conditions. However, unlike linear poroelasticity, in our models, pore pressure varies also with deviatoric stresses, where rising deviatoric stresses (at constant mean stress) depress pore pressure due to dilatancy. We showed that the model with N_1 leads to constant Skempton coefficients, A and B , with A smaller than $1/3$. This result in isotropic medium is in agreement with the classic work of Skempton [8], Henkel [34], and Henkel and Wade [35], but does not fit well with the measured undrained response of sandstones (Figs. 2 and 3). The model version with N_2 , which leads to non-constant Skempton coeffi-

cients, can accommodate the experimentally observed variation of pore pressure with shear stress. Our predictions on pore pressure were found to agree with undrained triaxial experiments on Berea and Navajo sandstones (Figs. 2 and 3). Nonlinear poroelastic response of Berea and Navajo sandstones was also observed in hydrostatic experiments [11,58]. However, in this paper we focus on the nonlinear poroelastic response to shear.

Pore pressure affects rock failure and plays an essential role in the seismic cycle. Hence, a mechanism of pore pressure increase was suggested for weakening major fault zones [4,5]. By contrast, pore pressure decrease increases the Coulomb stress, and therefore acts to strengthen fault zones. The behavior of pore pressure presented in this paper can explain dilatancy hardening observed in undrained experiments of high-porosity rocks [11]. Hence we propose that dilatancy hardening should be taken into consideration in predictions of Coulomb failure stress of these rocks (Fig. 4). This behavior of pore pressure can also increase Coulomb failure stress of high-porosity gouge, a significant component of major fault zones.

We have presented an application to coseismic distribution of pore pressure changes around a strike-slip fault. The pattern of pore pressure changes calculated using our model in high-porosity rocks is quite different from that predicted by linear poroelasticity (Fig. 5). Owing to the shear-dilation coupling term (N_2) in the poroelastic potential (Eq. (13)), the area of pore pressure decrease in our model is significantly larger than expected from linear poroelasticity. Therefore, shear-dilation coupling may be the reason for the observed pore pressure changes that cannot be explained by linear poroelasticity [9,10], and for the observed coseismic water level changes in regions of high shear but small volumetric strain expected from linear poroelasticity [1,59]. This calculation shows that the incorporation of nonlinear poroelastic coupling can have important consequences for estimating coseismic water level changes and crustal deformation driven by pore pressure diffusion.

Acknowledgments

We thank D.A. Lockner for useful discussions, and V. Courtillot and two anonymous reviewers for con-

structive reviews. Y. Hamiel and V. Lyakhovsky acknowledge support from the US–Israel Binational Science Foundation, grant BSF-9800198. V. Lyakhovsky thanks ISF 479/03, and A. Agnon thanks EU-INTAS grant # 0748 for support.

Appendix A

In this appendix we present the basic equations used to calculate Skempton coefficients A (or A') and B . In order to evaluate the poroelastic coefficients we differentiate the pore pressure with respect to σ_m and τ_{oct} (Eq. (11)). Since the nonlinear free energy (Eq. (13)) is expressed in terms of the strain invariants we write σ_m and τ_{oct} as function of these invariants. Using the definitions for σ_m (text before Eq. (6)) and τ_{oct} (Eq. (10)), they can be written as

$$\sigma_m = -\left(K - \frac{\gamma'}{\xi^*}\right)I_1 + \beta M(-\beta I_1 + \zeta), \quad (\text{A1})$$

$$\tau_{\text{oct}}^2 = \frac{4}{3}\left(\mu - \frac{1}{2}\gamma'\xi^*\right)^2\left(I_2 - \frac{1}{3}I_1^2\right), \quad (\text{A2})$$

for the model with the non-Hookean term N_1 (Eq. (15a)); and,

$$\sigma_m = -\left(K - \gamma\left(\frac{1}{\xi} + \frac{\zeta}{3}\right)\right)I_1 + \beta M(-\beta I_1 + \zeta), \quad (\text{A3})$$

$$\tau_{\text{oct}}^2 = \frac{4}{3}\left(\mu - \frac{1}{2}\gamma\xi\right)^2\left(I_2 - \frac{1}{3}I_1^2\right), \quad (\text{A4})$$

for the model with the non-Hookean term N_2 (Eq. (15b)). Under undrained conditions ($\zeta=0$) the state of our system is completely defined by the two strain invariants I_1 and I_2 . Therefore, using (Eq. (11)) A' and B can be written as

$$A' = \frac{(\partial p/\partial I_1)dI_1}{(\partial \tau_{\text{oct}}/\partial I_1)dI_1 + (\partial \tau_{\text{oct}}/\partial I_2)dI_2} \Bigg|_{\sigma_m}, \quad (\text{A5})$$

$$B = \frac{(\partial p/\partial I_1)dI_1}{(\partial \sigma_m/\partial I_1)dI_1 + (\partial \sigma_m/\partial I_2)dI_2} \Bigg|_{\tau_{\text{oct}}}. \quad (\text{A6})$$

In the case of constant σ_m , dI_2 is given as

$$dI_2 = - \frac{(\partial \sigma_m / \partial I_1)}{(\partial \sigma_m / \partial I_2)} dI_1. \quad (\text{A7})$$

Whereas, constant τ_{oct} leads to

$$dI_2 = - \frac{(\partial \tau_{\text{oct}} / \partial I_1)}{(\partial \tau_{\text{oct}} / \partial I_2)} dI_1. \quad (\text{A8})$$

Combining Eqs. (A5) and (A7) yields

$$A' = \frac{(\partial p / \partial I_1)}{(\partial \tau_{\text{oct}} / \partial I_1) - (\partial \tau_{\text{oct}} / \partial I_2) \frac{(\partial \sigma_m / \partial I_1)}{(\partial \sigma_m / \partial I_2)}}, \quad (\text{A9})$$

Similarly to Eq. (A9), combining Eqs. (A6) and (A8) yields

$$B = \frac{(\partial p / \partial I_1)}{(\partial \sigma_m / \partial I_1) - (\partial \sigma_m / \partial I_2) \frac{(\partial \tau_{\text{oct}} / \partial I_1)}{(\partial \tau_{\text{oct}} / \partial I_2)}}. \quad (\text{A10})$$

Using Eqs. (A9) and (A10), and the expressions for σ_m (Eqs. (A1), (A3)), τ_{oct} (Eqs. (A2), (A4)), and p (Eq. (3)), A' and B can be written as Eqs. (21) and (22) for the model with the nonlinear term N_1 , and as Eqs. (26) and (30) for the model with the nonlinear term N_2 .

References

- [1] E. Quilty, E. Roeloffs, Water-level changes in response to the 20 December 1994 earthquake near Parkfield, California, *Bull. Seismol. Soc. Am.* 87 (1997) 310–317.
- [2] G. Pelzer, P. Rosen, F. Rogez, K. Hudnut, Postseismic rebound in fault step-overs caused by pore fluid flow, *Science* 273 (1996) 1202–1204.
- [3] S. Jonsson, P. Segall, R. Pederson, G. Björnsson, Post-earthquake ground movements correlated to pore-pressure transients, *Nature* 424 (2003) 179–183.
- [4] J.D. Byerlee, Friction, overpressure and fault normal compression, *Geophys. Res. Lett.* 17 (1990) 2109–2112.
- [5] J.R. Rice, Fault stress states, pore pressure distribution, and the weakness of the San Andreas fault, in: B. Evans, T.-f. Wong (Eds.), *Fault Mechanics and Transport Properties of Rocks*, Academic Press, San Diego, CA, 1992, pp. 476–503.
- [6] S.A. Miller, Y. Ben-Zion, J.P. Burg, A three-dimensional fluid-controlled earthquake model: behavior and implications, *J. Geophys. Res.* 104 (1999) 10,621–10,638.
- [7] S.A. Miller, Properties of large ruptures and the dynamical influence of fluids on earthquakes and faulting, *J. Geophys. Res.* 107 (2002), doi:10.1029/2000JB000032.
- [8] A.W. Skempton, The pore-pressure coefficients A and B , *Geotechnique* 4 (1954) 143–147.
- [9] H.F. Wang, Effects of deviatoric stress on undrained pore pressure response to fault slip, *J. Geophys. Res.* 102 (1997) 17943–17950.
- [10] S. Ge, S.C. Stover, Hydrodynamic response to strike- and dip-slip faulting in a half-space, *J. Geophys. Res.* 105 (2000) 25513–25524.
- [11] D.A. Lockner, S.A. Stanchits, Undrained poroelastic response of sandstones to deviatoric stress change, *J. Geophys. Res.* 107 (2002), doi:10.1029/2001JB001460.
- [12] M.A. Biot, D.G. Willis, The elastic coefficients of the theory of consolidation, *J. Appl. Mech., Trans. ASME* 79 (1957) 596–601.
- [13] W.F. Brace, Some new measurements of the linear compressibility of rocks, *J. Geophys. Res.* 70 (1965) 391–398.
- [14] B.T. Brady, The non-linear behavior of brittle rock, *Int. J. Rock Mech. Min. Sci. Geomech. Abstr.* 6 (1969) 301–310.
- [15] D.R. Schmitt, M.D. Zoback, Diminished pore pressure in low-porosity crystalline rock under tensional failure: apparent strengthening by dilatancy, *J. Geophys. Res.* 97 (1992) 273–288.
- [16] P.A. Johnson, B. Zinszner, P.N.J. Rasolofosaon, Resonance and elastic nonlinear phenomena in rock, *J. Geophys. Res.* 101 (1996) 11553–11564.
- [17] E.H. Field, P.A. Johnson, I.A. Beresnev, Y. Zeng, Nonlinear ground-motion amplification by sediments during the 1994 Northridge earthquake, *Nature* 390 (1997) 599–602.
- [18] G. Peltzer, F. Crampe, G. King, Evidence of nonlinear elasticity of the crust from the Mw7.6 Manyi (Tibet) earthquake, *Science* 286 (1999) 272–276.
- [19] M. Nishihara, Stress–strain relation of rocks, *Doshisha Eng. Rev.* 8 (1957) 32–54.
- [20] J.B. Walsh, The effect of cracks on the uniaxial elastic compression of rocks, *J. Geophys. Res.* 70 (1965) 399–411.
- [21] M.D. Zoback, J.D. Byerlee, The effect of microcrack dilatancy on the permeability of Western granite, *J. Geophys. Res.* 80 (1975) 752–755.
- [22] D.A. Lockner, J.D. Byerlee, Development of fracture planes during creep in granite, in: H.R. Hardy, F.W. Leighton (Eds.), *2nd Conference on Acoustic Emission/Microseismic Activity in Geological Structures and Materials*, Trans-Tech. Publications, Clausthal-Zellerfeld, Germany, 1980, pp. 1–25.
- [23] R. Weinberger, Z. Reches, A. Eidelman, T.S. Scott, Tensile properties of rocks in four-point beam tests under confining pressure, in: P. Nelson, S.E. Laubach (Eds.), *Proceedings First North American Rock Mechanics Symposium*, Austin, Texas, 1994, pp. 435–442.
- [24] R.N. Schock, The response of rocks to large stresses, in: D.L. Roddy, R.O. Pepin, R.B. Merrill (Eds.), *Impact and Explosion Cratering*, Pergamon Press, New York, 1977, pp. 657–688.
- [25] M.S. Paterson, *Experimental Rock Deformation—The Brittle Field*, Springer-Verlag, Berlin, 1978, 254 pp.
- [26] K. Terzaghi, *Erdbaumechanik auf bodenphysikalischer Grundlage*, Deuticke, Leipzig, 1925, 399 pp.
- [27] M.A. Biot, General theory of three-dimensional consolidation, *J. Appl. Phys.* 12 (1941) 155–164.

- [28] V.N. Nikolaevsky, K.S. Vasniev, A.T. Gorbunov, G.A. Zotov, *Mechanics of Saturated Porous Media*, Nedra, Moscow, 1970, 342 pp. (in Russian).
- [29] A. Nur, J.D. Byerlee, An exact effective stress law for elastic deformation of rock with fluids, *J. Geophys. Res.* 76 (1971) 6414–6419.
- [30] J.R. Rice, M.P. Cleary, Some basic stress diffusion solution for fluid-saturated elastic porous media with compressible constituents, *Rev. Geophys. Space Phys.* 14 (1976) 227–241.
- [31] M.A. Biot, General solutions of the equations of elasticity and consolidation for a porous material, *J. Appl. Mech.* 78 (1956) 91–96.
- [32] L.E. Malvern, *Introduction to the Mechanics of a Continuum Medium*, Prentice-Hall, Inc., Englewood Cliffs, New Jersey, 1969, 713 pp.
- [33] O. Coussy, *Mechanics of Porous Continua*, Wiley, Chichester, 1995, 455 pp.
- [34] D.J. Henkel, The shear strength of saturated remoulded clays, *Proceedings of the American Society of Civil Engineers Research Conference on Shear Strength of Cohesive Soils*, Am. Soc. Civ. Eng., New York, 1960, pp. 533–554.
- [35] D.J. Henkel, N.H. Wade, Plane strain tests on a saturated remolded clay, *J. Soil Mech. Found. Div.* 92 (1966) 67–80.
- [36] J.C. Jaeger, N.G.W. Cook, *Fundamentals of Rock Mechanics*, Chapman and Hall, New York, 1984, 593 pp.
- [37] D.A. Lockner, J.D. Byerlee, Dilatancy in hydraulically isolated faults and the suppression of instability, *Geophys. Res. Lett.* 21 (1994) 2353–2356.
- [38] M.A. Biot, Nonlinear and semilinear rheology of porous solids, *J. Geophys. Res.* 78 (1973) 4924–4937.
- [39] F.D. Murnaghan, *Finite Deformation of an Elastic Solid*, John Wiley, Chapman, New York, 1951, 140 pp.
- [40] K. Brugger, Thermodynamic definition of higher order elastic constants, *Phys. Rev.* 133 (1964) 1611–1612.
- [41] F. Birch, Elasticity and constitution of the Earth's interior, *J. Geophys. Res.* 57 (1952) 227–286.
- [42] P.A. Johnson, P.N.J. Rasolofosaon, Nonlinear elasticity and stress-induced anisotropy in rock, *J. Geophys. Res.* 101 (1996) 3113–3124.
- [43] V. Lyakhovskiy, Z. Reches, R. Weinberger, T.E. Scott, Nonlinear elastic behavior of damaged rocks, *Geophys. J. Int.* 130 (1997) 157–166.
- [44] N.R. Hansen, H.L. Schreyer, A thermodynamically consistent framework for theories of elasticity coupled with damage, *Int. J. Solids Struct.* 31 (1994) 359–389.
- [45] V.A. Lyakhovskiy, V.P. Myasnikov, On the behavior of visco-elastic cracked solid, *Phys. Solid Earth* 4 (1985) 28–35.
- [46] V. Lyakhovskiy, Y. Podladchikov, A. Poliakov, A rheological model of a fractured solid, *Tectonophysics* 226 (1993) 187–198.
- [47] V. Lyakhovskiy, V. Myasnikov, Acoustics of rheologically nonlinear solids, *Int. J. Phys. Earth Planet. Int.* 50 (1988) 60–64.
- [48] V. Lyakhovskiy, V. Myasnikov, Relation between seismic wave velocity and state of stress, *Geophys. J. R. Astron. Soc.* 2 (1987) 429–437.
- [49] B. Budiansky, R.J. O'Connell, Elastic moduli of a cracked solid, *Int. J. Solids Struct.* 12 (1976) 81–97.
- [50] Y. Hamiel, V. Lyakhovskiy, A. Agnon, Coupled evolution of damage and porosity in poroelastic media: theory and applications to deformation of porous rocks, *Geophys. J. Int.* 156 (2004) 701–713.
- [51] R.A. Harris, Introduction to special section: stress triggers, stress shadows, and implications for seismic hazard, *J. Geophys. Res.* 103 (1998) 24,347–24,358.
- [52] N.M. Beeler, R.W. Simpson, S.H. Hickman, D.A. Lockner, Pore fluid pressure, apparent friction, and Coulomb failure, *J. Geophys. Res.* 105 (2000) 25,533–25,542.
- [53] J.D. Byerlee, Frictional characteristics of granite under high confining pressure, *J. Geophys. Res.* 72 (1967) 3639–3648.
- [54] M. Cocco, J.R. Rice, Pore pressure and poroelasticity effects in Coulomb stress analysis of earthquake interactions, *J. Geophys. Res.* 107 (2002), doi:10.1029/2000JB000138.
- [55] Y. Hamiel, Y. Liu, V. Lyakhovskiy, Y. Ben-Zion, D. Lockner, A visco-elastic damage model with applications to stable and unstable fracturing, *Geophys. J. Int.* 159 (2004) 1155–1165.
- [56] P.A. Cundall, Numerical experiments on localization in frictional materials, *Ign. Arch.* 59 (1989) 148–159.
- [57] P.A. Cundall, M. Board, A microcomputer program for modeling large-strain plasticity problems, in: C. Swoboda (Ed.), *Numerical Methods in Geomechanics*, Proc. 6th Int. Conf. Numerical Methods in Geomechanics, Innsbruck, Balkema, Rotterdam, 1988, pp. 2101–2108.
- [58] D.J. Hart, H.F. Wang, Pore pressure and confining stress dependence of poroelastic linear compressibilities and Skempton's B coefficient for Berea sandstone, in: B. Amadei, R.L. Kranz, G.A. Scott, P.H. Smeallie (Eds.), *Rock Mechanics for Industry*, Proc. 37th U.S. Rock Mechanics Symposium, Balkema, Rotterdam, 1999, pp. 365–371.
- [59] G. Grecksch, F. Roth, H.J. Kumpel, Coseismic well-level changes due to the 1992 Roermond earthquake compared to static deformation of half-space solutions, *Geophys. J. Int.* 138 (1999) 470–478.